Drug Design, Development and Therapy

Dovepress
Taylor & Francis Group

Open Access Full Text Article

ORIGINAL RESEARCH

Ursolic Acid Ameliorates Diabetic Nephropathy by Inhibiting JAK2/STAT3-Driven Ferroptosis: Mechanistic Insights from Network Pharmacology and Experimental Validation

Yijing Zhou*, Chengli Lou*, Xiuqin Xu, Bo Feng, Xiaoping Fan, Xiangjing Wang

Department of Nephropathy, Jiaxing Traditional Chinese Medicine Hospital, Jiaxing, People's Republic of China

*These authors contributed equally to this work

Correspondence: Yijing Zhou, Email zyj13967332522@163.com

Purpose: Ursolic acid (UA) improves diabetic nephropathy (DN), but its regulatory mechanism requires further verification.

Methods: The bioactive component-target network of UA in DN was determined using a network pharmacology approach. DN mice (STZ-diabetic C57BL/6 mice, n = 8/group, 4 weeks) were treated with UA (25 mg/kg and 100 mg/kg) and the JAK agonist RO8191 (2 mg/kg). The DN cell model (high glucose-injured NRK-52E cells) was treated with UA (10 and 50 μM) and RO8191 (2 μM) for 24 h. The molecular mechanisms by which UA acts were further verified in vivo and in vitro.

Results: UA treatment ameliorated the general state of the DN mouse model, as characterized by the attenuation of weight loss and downregulation of fasting blood glucose (FBG) and fasting serum insulin (FINS) levels (all $P < 0.05$). Renal pathological changes and impaired renal function (increased levels of Scr, BUN, and UAER) were also improved by UA treatment (all $P < 0.05$). In vitro, UA increased the viability of DN cells in vitro ($P < 0.001$). Concurrently, UA remarkably downregulated the levels of ROS, SOD, and iron and up-regulated the levels of MDA, GPX4, and SLC7A11 (all $P < 0.05$) in vivo and in vitro. Mechanistically, activation of the JAK2-STAT3 pathway with the agonist RO8191 significantly reduced UA's anti-ferroptosis and anti-oxidative effects of UA.

Conclusion: UA protected against DN by blocking JAK2/STAT3-mediated ferroptosis.

Keywords: diabetic nephropathy, ursolic acid, JAK2/STAT3 pathway, ferroptosis, network pharmacology

Introduction

Diabetes is a global challenge that affects 425 million people, and the International Diabetes Federation predicts that the number of patients with diabetes will increase to 700 million by 2045.[1,2] Diabetic nephropathy (DN) is a serious complication of diabetes. The global prevalence of DN is estimated to be approximately 40% in patients with diabetes and still has an annual upwards trend.[3] DN leads to the incidence and mortality of cardiovascular diseases, resulting in a huge socioeconomic burden.[4,5] The pathophysiology of DN involves a number of physiological imbalances, including metabolic anomalies, renin-angiotensin system activation, oxidative stress, hemodynamic irregularities, and fibrosis.[6,7] Strict control of blood pressure, administration of angiotensin-converting enzyme inhibitors, and inhibition of the renin-angiotensin system can alleviate the symptoms of DN. However, there are no effective drugs to prevent and treat DN.[8] Therefore, it is important to understand the pathogenesis of DN to identify new drug targets.

Recently, research on the therapeutic effects and mechanisms of herbal medicines and their active ingredients on diseases including DN has received widespread attention.[9] Ursolic acid (UA) has been proven to exert biological activity in different types of diseases such as cancer, neuronal damage, intestinal injury, liver fibrosis, and kidney diseases.[10–13] Various studies have indicated that UA has low toxicity in clinical application and exhibits numerous bioactive activities,

Received: 26 March 2025
Accepted: 17 July 2025
Published: 4 August 2025

including anti-inflammatory, anti-oxidative, and inhibiting cell apoptosis.[14] In clinical practice, UA is used in conjunction with chemotherapeutic agents to enhance their anticancer effects and improve safety.[15] For DN, although the therapeutic effect of UA on patients with DN and its renal toxicity to patients have not been reported, many researchers have confirmed the therapeutic effect and safety of UA on DN through mouse and cell experiments.[16] Wu and his partners treated a DN rat model with 50 mg/kg UA. They found that UA could alleviate the increases in blood glucose, inflammatory factors, and oxidation factors in a DN rat model.[16] UA has also been reported to improve DN by inhibiting oxidative stress and inflammation in streptozotocin (STZ)-induced rats.[17] For combination therapy, Yang et al also reported that the combined use of UA with insulin has a mitigating role in apoptosis and oxidative stress in DN in type 1 diabetes mellitus (T1DM) rats.[18] Nonetheless, the deep mechanism of UA in regulating inflammation and oxidative stress in DN requires further exploration.

As an iron-dependent non-apoptotic form of cell death, ferroptosis is suggested to be a strong link with the complications of diabetes.[19] Iron deposition in cells contributes to the accumulation of reactive oxygen species (ROS) and ROS-induced oxidative stress, further enhancing lipid peroxidation, which is a key factor of ferroptosis.[20] High glucose attracts Fe^{2+} overload and Fe^{2+} imbalance, then enhancing ROS production and oxidative stress, which further causes ferroptosis,[21] and in patients with diabetes, hyperglycemia causes excessive production of ROS and gives rise to oxidative stress injury in various organs.[22] In recent years, many researchers have also used ferroptosis as a new strategy for traditional Chinese medicine (TCM) treatment of DN.[23] Some bioactive components of TCM such as Glabridin and Vitexin, have been found to ameliorate DN via suppressing ferroptosis.[24,25] The above research indicates that reducing ferroptosis could be a prospective therapeutic method for DN. However, there is no evidence of the regulatory role of UA in ferroptosis in DN. Therefore, the molecular mechanism by which UA modulates ferroptosis in DN remains to be elucidated.

Janus Kinase (JAK) belong to the tyrosine kinase family, and the signal transducer and activator of transcription (STAT) signaling pathway is a downstream signaling pathway activated by JAKs.[26] The JAK/STAT pathway is critical in regulating gene expression and cellular activation, proliferation, and differentiation in response to cytokines and other stimuli.[27] The JAK/STAT pathway is activated in DN, of which the JAK2/STAT3 subtype is the most widely and intensively studied.[28] Isoliquiritigenin (ISL) displayed preventive effects on high glucose (HG)-exposed GMCs through inhibiting JAK2/STAT3 pathway and provided an insight into the application of ISL for DN treatment.[29] Administration of Boeravinone B showed renal protective effects against STZ-induced DN in rats via the reduction of oxidative stress, inflammatory reactions and JAK2/STAT3 pathway.[30] The relationship between the JAK2/STAT3 pathway and ferroptosis is also gaining attention. STAT3 inhibitors can block FPN1 degradation, thereby promoting iron export, reducing iron deposition, significantly lowering ROS and malondialdehyde (MDA) levels, and restoring glutathione peroxidase 4 (GPX4) and GSH levels. In turn, the accumulation of iron ions can activate the JAK2/STAT3 pathway.[31] More importantly, UA was found to induce apoptosis in colorectal cancer cells partially via upregulation of miR-4500 and inhibition of JAK2/STAT3 phosphorylation.[32] Therefore, this study hypothesized that UA might ameliorate DN by inhibiting ferroptosis by regulating the JAK2/STAT3 pathway.

To explore the underlying mechanism by which UA improves DN, we employed a comprehensive approach that combined network pharmacology analysis with experimental validation. We induced DN in a mouse model using a high-fat diet (HFD) and STZ. High glucose-induced NRK-52E cells were used for the in vitro studies. Through Network pharmacology and enrichment analysis, we found that the potential targets of UA in DN were closely related to ferroptosis and were concentrated in the JAK2/STAT3 signaling pathway. Experimental verification showed that UA effectively mitigated ferroptosis and improved DN by inhibiting the JAK2/STAT3 pathway in vivo and in vitro. These findings are expected to provide further support for the traditional use of UA in DN treatment.

Materials and Methods

Animals and Experimental Design

Six-week-old male C57BL/6 mice at 6 weeks old were purchased from Cavens (Changzhou, China). UA (purity: 98.5%, analytical standard) was purchased from Sigma-Aldrich (89797, St. Louis, MO, USA). The animal trial was approved by the Ethics Committee of Jiaxing Traditional Chinese Medicine Hospital (approval number: JUMC2025-029). During the

experiments, all mice were housed in an animal room with a 12-h light/dark cycle. All the animals were permitted to eat and drink at any time. All animal experiments were performed and analyzed in a blinded manner. The DN model was established as previously reported.[33] In brief, mice were received with a HDF (D12492, Research Diets, New Brunswick, New Jersey, USA) which contained about 45% fat, 35% protein, and 20% carbohydrates for 4 weeks. After 4 weeks of HDF, all mice were administered 100 mg/kg STZ (S8050, Solarbio, Beijing, China) once via intraperitoneal injection. Ten days after STZ injection, blood samples from the tail vein of mice were collected for fasting blood glucose (FBG) detection using a blood glucose monitoring system (ACCU-CHEK Performa; Roche, Basel, Switzerland). Urine was collected, and 24-h urine protein levels were measured using a commercial enzyme-linked immunosorbent assay (ELISA) kit (ml025062; Mlbio, Shanghai, China). Mice with the random FBG levels from 7.8 mM to 16.67 mM and random urine protein levels of ≥20 mg/24 h identified as DN mice model were selected and included in the experiment. These mice were identified as a DN mouse model.

There were two parts to the animal experiment. First, mice were randomly divided into four groups (n = 8/group, 4 weeks): the control, DN, DN+UA-L, and DN+UA-H groups. The mice in the control group were fed a normal diet. Mice in the DN, DN+UA-L, and DN+UA-H groups were used as the DN mouse model. In addition, mice in the DN +UA-L and DN+UA-H groups were then orally administered 25 mg/kg and 100 mg/kg UA (U8220, Solarbio) once a day for 4 weeks.[16,18] The dose of UA administered was obtained from the appropriate literature.[16,34–36]

For the second part, the mice in the second part were randomly divided into 4 groups (STZ-diabetic C57BL/6 mice, n = 8/group, 4 weeks): the DN group, the DN+UA-H group, the DN+RO8191 group, and the DN+UA-H+RO8191 group. Mice in the DN+UA-H group were orally received 100 mg/kg UA once a day for 4 weeks, and mice in the DN+RO8191 group were intraperitoneal received 2 mg/kg JAK agonist RO8191 (IR1400, Solarbio) once a day for 4 weeks,[37] mice in the DN+UA-H+RO8191 group were orally received 100 mg/kg UA and intraperitoneal administrated 2 mg/kg RO8191 once a day for 4 weeks.

During the 4 weeks of UA and RO8191 treatment, the body weight and food and water intake of all mice were documented. Within 24 h before the end of the experiments, urine samples of all mice were collected, and alloknesis assessment was conducted on all mice. On the last day of the experiments, tail vein blood samples of all mice were collected after the mice were fasted overnight fasting. Finally, all mice were sacrificed by cervical dislocation after pentobarbital sodium injection, and their pancreas and kidney tissues were collected and weighed for later analysis.

Alloknesis Assessment

As previously reported,[38] alloknesis testing was performed on all mice. Briefly, a 0.7 mN von Frey filament (NC12775, Yuyan, Shanghai, China) was used to induce scratching responses in the neck area of all mice, and the alloknesis score was examined by documenting the scratching numbers.

Detection of Biochemical Indicators and Kidney Index

Serum was collected by centrifuging the tail vein blood samples for 20 min at 3000 rpm and 4°C. FBG levels were then examined using a glucose monitoring system, and fasting serum insulin (FINS) levels were measured using an enzyme-linked immunosorbent assay (ELISA) kit for mouse insulin (SEKM-0141, Solarbio) according to the manufacturer's instructions. Then, the value of insulin resistance (HOMA-IR) and the value of homeostasis model assessment of β-cell function (HOMA-β) were calculated using the formula HOMA-IR= (FINS × FBG)/22.5 and HOMA-β = 20 × FINS/(FBG-3.5).[24]

After the kidneys of all mice were obtained and weighed, the kidney index was calculated using the following formula: kidney index = kidney weight/body weight. Renal function factors, including urinary albumin excretion rate (UAER), serum creatinine (Scr), blood urea nitrogen (BUN), and 24-h urine protein, were determined using the Scr detection kit (E-BC-K188 -M, Elabscience, Wuhan, China), UAER detection kit (E-EL-M3032, Elabscience), BUN detection kit (E-BC-K183-M, Elabscience), and urine protein detection kit (ml025062, Mlbio, Shanghai, China), respectively.

Hematoxylin-Eosin (HE) Staining

The HE Staining Kit (C0105S) was purchased from Beyotime (Shanghai, China). The pancreas and kidney tissues were fixed with 10% formalin fixative (IF9010, Solarbio) for 24 h. Then, the tissues were incubated with xylene (W14277,

Yuanye, Shanghai, China) and gradient alcohol. Subsequently, paraffin (V33396, Yuanye) was used to embed the tissues, which were further cut into 4 μm tissue slices and dewaxed. After the tissue slices were stained with hematoxylin for 10 min, hydrochloric acid alcohol (R33067, Yuanye) for 2s, and eosin for 1 min, they were subsequently treated with xylene and neutral gum (S30509, Yuanye). Finally, a microscopic imaging system (THUNDER, Leica, Wetzlar, Germany) was used to observe the histopathology of pancreas and kidney tissues.

Masson Staining

Kidney tissue fibrosis was detected using a Masson staining kit (G1340, Solarbio). Briefly, the tissue slice was first incubated with Weigert iron hematoxylin staining buffer for 5 min and acid ethanol for 8s, followed by washing with double distilled water for 30s. Then, the tissue was incubated with Masson Blue reagent for 5 min and washed with double distilled water for 30s. Later, a Ponceau fuchsin staining solution was used to treat the tissue for 10 min and a weak acid working buffer was used to wash the tissue for 30s. After treatment with aniline blue staining reagent for 2 min and rinsing with a weak acid working buffer for 30s, the tissue was further treated with xylene and neutral gum. Finally, a THUNDER microscope was used to observe the tissue samples. Images were analyzed using Image-Pro Plus software ((National Institutes of Health, Bethesda, MD, USA)) to assess the degree of fibrosis in the kidney tissue.

Acquisition of Therapeutic Targets for DN and UA

The GeneCards database (https://www.genecards.org/) was searched for DN-related genes. UA was searched as a search term sequentially in the Swisstarget database (http://www.swisstargetprediction.ch), Targetnet database (http://targetnet.scbdd.com), and Traditional Chinese Medicine Systems Pharmacology (TCMSP) database (https://old.tcmsp-e.com/tcmsp.php) to identify the therapeutic targets of UA. The therapeutic targets of UA were obtained after removing duplicate values.

UA Therapeutic Targets and DN Marker Overlap

Finally, based on the targets of UA and disease genes in DN, the common targets (potential targets of UA in treating DN) were identified and exhibited with a Venn diagram using the Venny 2.1 website (https://bioinfogp.cnb.csic.es/tools/venny/).

Construction of Protein-Protein Interaction (PPI) Network

The potential targets of UA in treating DN were put into the STRING platform (https://cn.string-db.org/cgi/input.pl), the PPI network was constructed hiring the condition of "Multiple proteins" and "Homo sapiens" and the software of Cytoscape 3.9.1 (National Institute of General Medical Sciences, Bethesda, MD, USA). Centiscape 2.2 plugin was used to calculate the closeness, degree, and betweenness between nodes and hub genes.

Enrichment Analyses of Gene Ontology (GO) and Kyoto Encyclopedia of Genes and Genomes (KEGG)

Using the DAVID database (https://david.ncifcrf.gov/home.jsp), GO function and KEGG pathway enrichment analyses of hub genes were performed to explore the biological function and pathways of UA in DN. During the analysis, the parameter 'species, "list type", and "identifier" were successively set to "Homo sapiens", "gene list", and "official gene symbol". A q value <0.05 or P value <0.05 was arranged in descending order. Sankey diagrams and bubble charts were constructed using R 4.2.0 software (Lucent Technologies, Murray Hill, NJ, USA).

Cell Culture and Induction

The rat kidney cell line NRK-52E (CL-0174) was obtained from Procell (Wuhan, China) and incubated in Dulbecco's modified Eagle's medium (DMEM) medium (PM150270, Procell) containing 10% fetal bovine serum (FBS; FB-1058, Biosun, Shanghai, China) and 1% penicillin-streptomycin solution (PS; P1400, Solarbio). NRK-52E cells were cultured at 37 °C in a saturated humid environment with 5% CO_2. The NRK-52E cells were epithelial cell-like and grew in an adherent shape. Upon reaching approximately 70–80% confluence, the cells were treated. To induce the DN cell model, NRK-52E cells were incubated in medium supplemented with 30 mM HG (HG-injured NRK-52E cells) (G8150,

Solarbio) for 48 h. Cells cultured in medium supplemented with 5 mM glucose were regarded as the control group.[39] For UA treatment, after HG treatment, NRK-52E cells were treated with UA-L (10 μM) and UA-H (50 μM) for 24 h. For the JAK agonist RO8191 treatment, after HG treatment, NRK-52E cells were treated with 2 μM RO8191 for 24 h.[37]

Detection of Cell Viability

After HG administration, NRK-52E cells were collected and placed in 96-well plates. Each well of a 96-well plate contained 3×10^3 cells in 100 μL of complete medium with or without UA. After the cells were further treated with UA for 24 h in a 96-well plate, the culture medium was changed with a mixed solution of 90 μL DMEM medium and 10 μL detection reagent of cell counting kit-8 (CCK-8) (CA1210, Solarbio) for 1 h of incubation. Finally, the optical density (OD) of NRK-52E cells in each well was examined using a Varioskan LUX microplate reader (Thermo, Waltham, Massachusetts, USA) at 450 nm to evaluate cell viability.

Detection of ROS Level

ROS levels in NRK-52E cells and mouse kidneys were measured by flow cytometry using an ROS assay kit (50101ES01, Yeasen, Shanghai, China). In brief, NRK-52E cells and kidney tissue homogenates were administered with 10 μM DCFH-DA reagent, and DCFH-DA was pre-diluted in DMEM without FBS at a dilution ratio of 1:1000. After 20 min of incubation at 37°C, the samples were washed four times with FBS-free DMEM. The samples were then analyzed using an Attune NxT flow cytometer (Thermo).

Assessment of Oxidative Stress

The levels of superoxide dismutase (SOD), MDA, and iron in the NRK-52E cells and mouse kidneys were evaluated. An MDA detection kit (ADS1001W196, AIDISHENG, Jiangsu, China), total SOD detection kit (50104ES60, Yeasen), and iron assay kit (ml095093, MlBio, Shanghai, China) were used to examine the levels of MDA, SOD, and iron in NRK-52E cells and kidney tissue homogenates according to the manufacturer's instructions.

Quantification of Protein Expression

Protein expression was determined by Western blotting. Briefly, the total proteins in the NRK-52E cells and mouse kidney tissues were obtained using the RIPA reagent (89901, Thermo), and the protein concentration was detected using a BCA detection kit (MA0082, MeilunBio, Dalian, China). SDS-PAGE gel was prepared using Acryl/Bis 40% Solution (B546014, Sangon Biotech, Shanghai), Tris-HCl Buffer (B546019, Sangon Biotech), and TEMED (A100761-0025, Sangon Biotech). The protein was denatured at 100°C for 5 min together with a loading buffer (S750306, Aladdin, Shanghai, China) and electrophoresed on an SDS-PAGE gel. After the protein in the SDS-PAGE gel was transferred to a hydrophilic PVDF membrane (H492770, Aladdin), which was pre-activated using soaking and activation buffer (S743277, Aladdin), the membrane was incubated with 5% defatted milk for 2 h. Later, the membrane was incubated with relative primary antibody for 16 h at 4°C and secondary antibody for 2 h. Finally, with the aid of electrochemiluminescence (ECL) liquid (180–501, Tanon, Shanghai, China), the membrane was visualized using an ECL instrument (Tanon 5200, Tanon). The antibodies used in this experiment were as follows: JAK2 (ab108596, dilution ratio 1:5000, Abcam, Cambridge, UK), p-JAK2 (ab219728, dilution ratio 1:3000, Abcam), STAT3 (STAT3; ab68153, dilution ratio 1:2000, Abcam), p-STAT3 (ab32143, dilution ratio 1:6000, Abcam), β-actin (ab8227, dilution ratio 1:5000, Abcam), and Goat Anti-Rabbit IgG H&L (HRP; ab6721, dilution ratio 1:15000, Abcam).

Quantification of Gene Expression

The expression of genes related to ferroptosis was determined using quantitative real-time PCR (qRT-PCR). Briefly, the total RNA in the NRK-52E cells and mice kidneys were obtained with the aid of an Trizol (15596026CN, Thermo), chloroform (10006818, Sinopharm (https://www.reagent.com.cn/), Shanghai, China), isopropanol (40064360, Sinopharm), absolute alcohol (10009218, Sinopharm), and DNase/RNase water (10977015, Thermo). The concentration of total RNA was determined using a UV spectrophotometer (NanoDrop; Thermo). cDNA was synthesized from the isolated RNA using a reverse transcription kit (R233-01, Vazyme, Nanjing, China) and mixed with SYBR qPCR Master

reagent (Q712-02, Vazyme), cDNA, and primers of the relative gene. Finally, the amplification reaction was performed using a 7500 qPCR System (Thermo). qPCR conditions were 95°C for 30s, 95°C for 10s, and 60°C for 30s (40 cycles). The mRNA level was normalized to the endogenous housekeeping gene β-actin and relative to the calibrator sample using the $2^{-\Delta\Delta CT}$ method.[40] The primers used in this experiment were shown in Supplementary Table 1 (Reference sequence of primers were shown in Supplementary data). The efficiency (e) of the PCR was calculated for each primer using the following formula: $e = 10^{\wedge}(1/-s) - 1$, where s is the slope of the standard curve, and only primers with efficiencies between 85 and 115% were used in this study.[24]

Statistical Analysis

Data were analyzed using SPSS 19 software (IBM, Armonk, New York, USA). The experiments in vivo were repeated eight times and the experiments in vitro were repeated five times to ensure reproducibility. The results are presented as mean ± standard deviation (SD). Normal distribution was first analyzed using the Shapiro–Wilk test, followed by the Levene test for homogeneity of variances. Data differences between groups were analyzed using two-tailed unpaired Student's *t*-tests or one-way ANOVA with Tukey's post hoc test. When the data deviated from a normal distribution, the non-parametric Kruskal–Wallis test was used. $P < 0.05$.

Results

UA Had an Anti-Hyperglycemic Effect on DN Mice

After the DN mouse model was treated with UA for four weeks, the parameters related to diabetes in all mice were examined. The body weight and intake of food and water from the mice in each group were documented once a week. The body weight of DN mice was reduced, but food and water intake increased from the second week to the fourth week ($P < 0.001$, Table 1). In addition, both 25 mg/kg UA treatment and 100 mg/kg UA treatment ameliorated the manifestations caused by DN ($P < 0.01$, Table 1). The FBG and FINS levels of the mice in each group were also examined. The results illustrated that FBG and FINS were elevated in DN mice compared to the mice in the control group ($P < 0.001$, Figure 1A and B). FBG and FINS levels were reduced in DN mice after both 25 and 100 mg/kg UA treatment ($P < 0.001$, Figure 1A and B). As expected, the reduced HOMA-β and increased HOMA-IR of DN mice were also reversed by treatment with 25 mg/kg UA and 100 mg/kg UA ($P < 0.001$, Figure 1C and D). Furthermore, histopathological analysis of mouse pancreas was performed using HE staining, as depicted in Figure 2; the interlobular area became wider, and vacuole loads were observed in the pancreatic tissue of DN mice, while the abnormal pancreatic

Table 1 The Body Weight, Food Intake and Water Intake of Mice

Group	n	0 W	1 W	2 W	3 W	4 W
Bodyweight (g)						
Control	8	17.59±0.30	18.60±1.05	20.95±0.44	24.81±1.29	25.75±1.69
DN	8	17.75±0.43	18.22±0.76	18.41±0.77***	18.02±1.24***	18.16±1.66***
DN+UA-L	8	17.57±0.18	17.90±0.83	18.91±1.10	20.33±1.66##	22.19±2.34####
DN+UA-H	8	17.62±0.30	18.80±0.47	20.10±0.32####	22.30±0.74####	24.03±0.80####
Food intake (g/day)						
Control	8	5.74±1.05	6.19±0.54	6.53±1.03	6.45±0.75	6.07±1.31
DN	8	5.78±1.03	6.47±0.81	9.50±1.51***	11.48±1.18***	11.69±1.75***
DN+UA-L	8	6.10±1.01	6.21±1.06	7.46±1.40##	9.29±1.24####	7.97±0.37####
DN+UA-H	8	6.23±0.53	6.30±1.10	7.35±0.51##	6.95±0.78####	6.56±1.27####
Water intake (mL/day)						
Control	8	8.58±0.49	8.20±0.56	8.24±0.59	8.88±0.54	8.15±0.95
DN	8	7.90±0.79	11.57±1.22***	13.70±2.01***	15.09±1.14***	18.55±2.26***
DN+UA-L	8	7.95±0.75	10.56±0.68	11.32±1.44##	11.30±1.20####	11.84±1.11####
DN+UA-H	8	7.75±1.29	9.06±1.23####	10.70±0.83####	10.93±0.59####	10.43±0.25####

Notes: Data are represented as mean ± SD (n=8). ***$P < 0.001$ vs Control; ##$P < 0.01$, ####$P < 0.001$ vs DN.

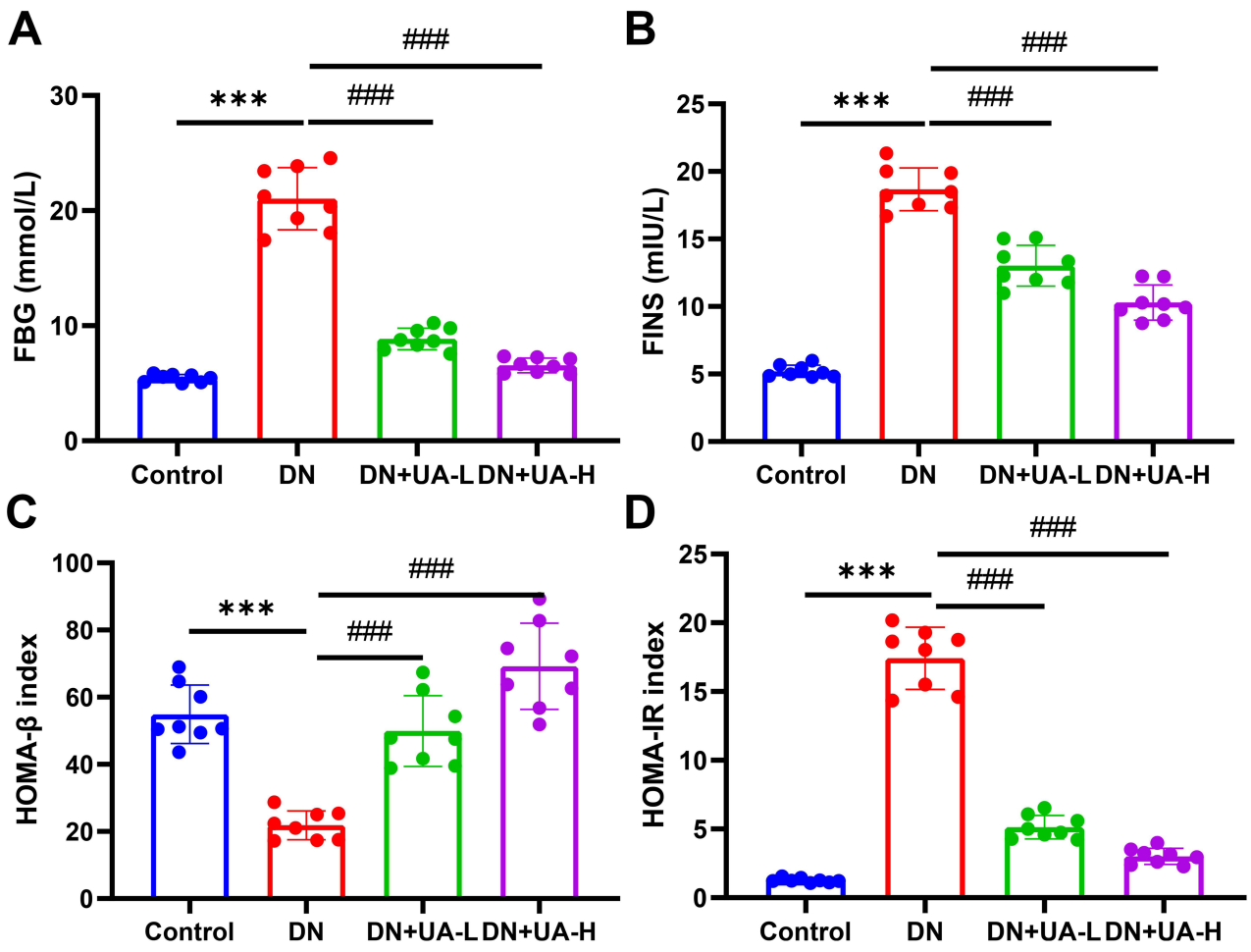

Figure 1 UA had an anti-hyperglycemic effect on DN mice. (**A**–**D**) After the DN mice model was established and the mice were treated with 25 mg/kg and 100 mg/kg UA for 4 weeks, the FBG (**A**) and FINS (**B**) of all mice were examined, the index of HOMA-β (**C**) and HOMA-IR (**D**) were calculated. Data are represented as mean ± SD (n=8). ***$P < 0.001$ vs Control; ###$P < 0.001$ vs DN.

Abbreviations: FBG, fasting blood glucose; DN, diabetic nephropathy; UA, Ursolic acid; FINS, fasting insulin; HOMA-β, homeostasis model assessment of β-cell function; HOMA-IR, the value of insulin resistance.

architecture changes in DN mice were restored after treatment with 25 mg/kg and 100 mg/kg UA. These findings revealed that UA plays an anti-hyperglycemic role in DN mice.

UA Had an Ameliorating Role in the Renal Dysfunction of DN Mice

Subsequently, indicators of renal function and renal histopathology of all mice were determined. As depicted in Figure 3A, glomerular nuclear overflow and tubular nuclear disorder in DN mice, while 25 mg/kg and 100 mg/kg UA treatment, improved these histopathological injuries in DN mice. Masson staining revealed that significant fibrosis occurred in the renal interstitium of DN mice, whereas after UA treatment, renal interstitial fibrosis in mice was mitigated (Figure 3B and Supplementary Figure 1). In addition, more itch behavior (Figure 4A), heavier kidney weight (Figure 4B), and higher kidney index (Figure 4C) were observed in DN mice than in control normal mice ($P < 0.001$). In addition, UA treatment reduced itch behavior, kidney weight, and kidney index of DN mice ($P < 0.001$, Figure 4A–C). Furthermore, the factors related to renal function, including Scr, BUN, UAER, and 24-h urine protein, were increased in DN mice ($P < 0.001$, Figure 4D–F and Supplementary Figure 2), and were then decreased by UA treatment ($P < 0.001$, Figure 4D–F and Supplementary Figure 2). These results indicate that renal function was impaired in DN mice, and UA had an ameliorating role in renal dysfunction in DN mice.

https://doi.org/10.2147/DDDT.S526554

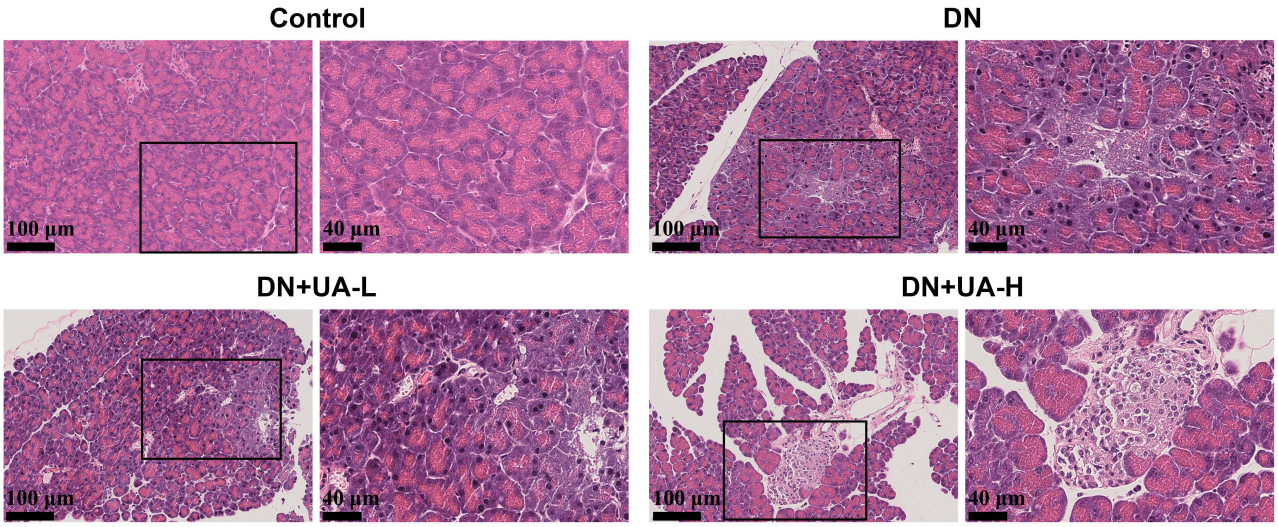

Figure 2 The histopathological of mice pancreas was detected through HE staining (scale bar = 100 μm (left) and 40 μm (right)); (n=8).
Abbreviations: DN, diabetic nephropathy; UA, Ursolic acid.

The Role of UA in the Treatment of DN Might Be Realized Through Ferroptosis and the JAK2/STAT3 Signaling Pathway

UA (Figure 5A) target genes were acquired through the TCMSP, Swisstarget, and Targetnet databases, and 509 valid genes were obtained after deleting duplicate values. Subsequently, we searched for DN-related genes using the Genecards database and obtained a total of 4806 genes. After overlapping the UA target genes and DN marker genes (Figure 5B), 301 valid genes were obtained. To explore the interactions of these 301 genes, they were imported into the STRING database to obtain a PPI network, which was subsequently analyzed in depth using the Cytoscape software (Figure 5C). To further clarify the potential therapeutic effect of UA on DN, these genes were imported into the DAVID database. Statistical significance was set at $P < 0.05$, and 10 entries from the GO and KEGG enrichment results were selected for presentation. According to the GO enrichment results, it may also be involved in biological processes such as "regulation of inflammatory response" and "response to oxygen levels" (Figure 6A). The UA-DN target may be a cellular component of the "oxidoreductase complex" (Figure 6B). It may also be involved in molecular function such as "dioxygenase activity" (Figure 6C). The KEGG enrichment results suggested that the mechanism of UA treatment for DN may involve the "JAK-STAT signaling pathway" and other pathways (Figure 6D), as shown in Figure 6E. These findings further revealed that the role of UA in the treatment of DN might be realized by regulating ferroptosis and the JAK/STAT signaling pathway.

UA Promoted the Cell Viability and Inhibited the Ferroptosis of DN Cell Model

CCK-8 assay was used to determine the appropriate concentration of UA in vitro. NRK-52E cells were exposed to different concentrations of UA for 24 h. UA at 400 μM had no effect on the viability of normal NRK-52E cells, suggesting that UA had virtually no drug toxicity ($P > 0.05$, Figure 7A). To verify the role of UA in the ferroptosis of DN, the HG induced NRK-52E cell model was established, and the cell model was further treated with UA. NRK-52E cell viability was found to have a marked increase at 10, 25, and 50 μM, compared to the HG group ($P < 0.001$, Figure 7B). Finally, 10 μM (UA-L) and 50 μM (UA-H) were selected as experimental drug concentrations. It was also found that HG increased the ROS level of NRK-52E cells ($P < 0.001$, Figure 7C), which was then reduced by UA-L and UA-H ($P < 0.001$, Figure 7C). In addition, the oxidative stress-related factors were evaluated, as illustrated in Figure 7D–F: HG induction reduced SOD levels and increased MDA and iron levels in NRK-52E cells ($P < 0.001$), and both UA-L and UA-H increased SOD levels and reduced the levels of MDA and iron in HG-treated NRK-52E cells (all $P < 0.05$). In addition, the expression of ferroptosis markers was further quantified, and the results showed that the levels of GPX4 and

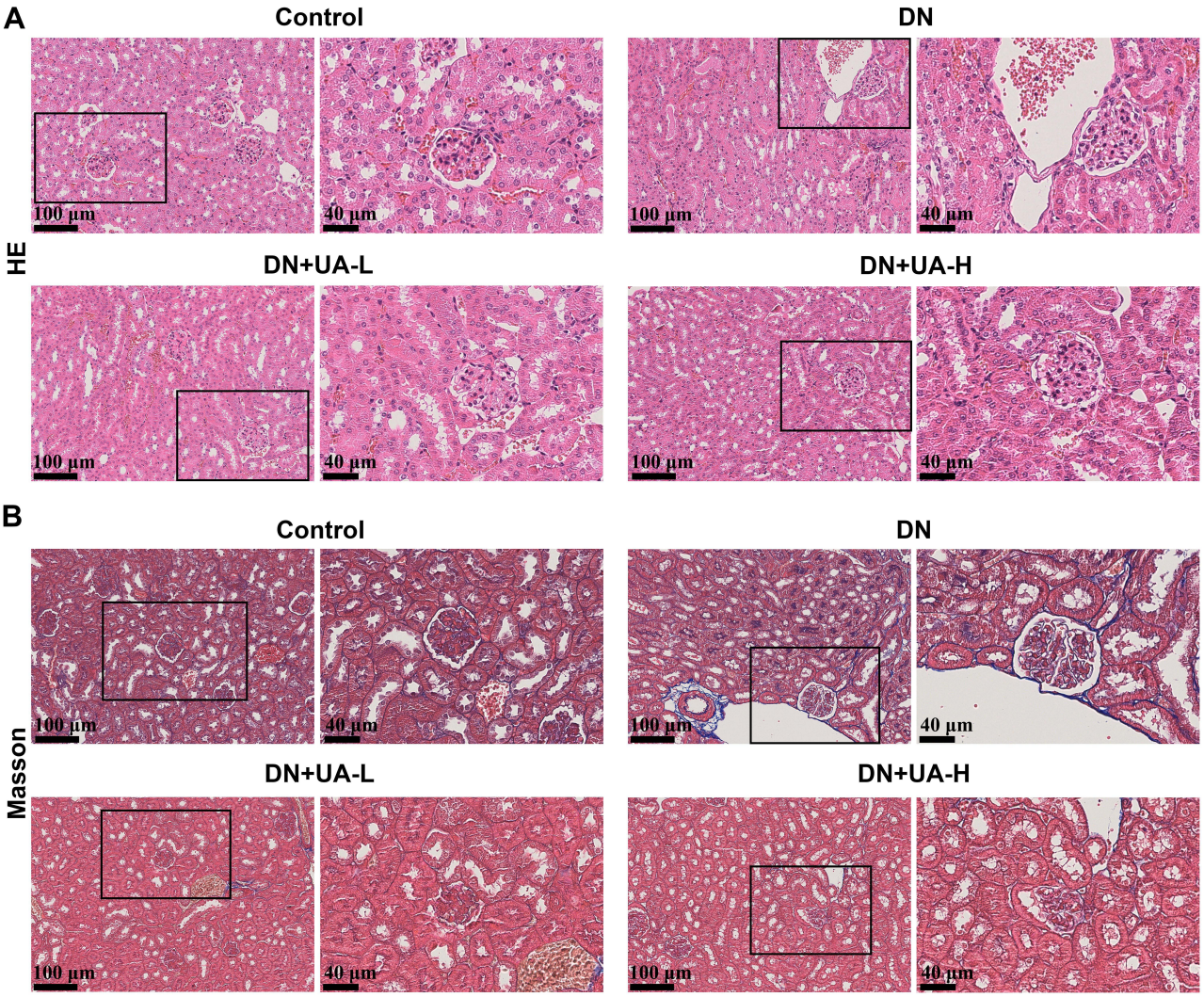

Figure 3 UA had an ameliorating role in the renal pathological changes of DN mice. (**A**) After the DN mice model was established and the mice were treated with 25 mg/kg and 100 mg/kg UA for 4 weeks, the renal histopathological of all mice were determined using HE staining (scale bar = 100 μm (left) and 40 μm (right)). (**B**) The kidney tissue fibrosis of all mice was examined using Masson staining (scale bar = 100 μm (left) and 40 μm (right)); (n=8).
Abbreviations: DN, diabetic nephropathy; UA, Ursolic acid; HE, Hematoxylin-eosin.

solute carrier family 7 member 11 (SLC7A11) in the HG-induced DN cell model were downregulated ($P < 0.001$, Figure 7G), which were then upregulated by UA-L and UA-H treatment (all $P < 0.05$, Figure 7G). The above evidence demonstrates that UA could promote cell viability and inhibit ferroptosis in a DN cell model.

UA Inhibited the Ferroptosis of DN Cell Model by Inhibiting the JAK2/STAT3 Pathway

Transduction of the JAK2/STAT3 pathway was detected. As shown in Figure 8A, the expression of p-JAK2 and p-STAT3 in NRK-52E cells was upregulated by HG induction. The upregulated levels of p-JAK2 and p-STAT3 in HG-treated cells were decreased by UA-L and UA-H (Figure 8A). To explore the regulatory role of UA in the JAK2/STAT3 pathway, NRK-52E cells were treated with 2 μM RO8191 24 h after HG induction. After RO8191 treatment, the oxidative stress and ferroptosis-related factors were then determined. As shown in Figure 8B–D, 50 μM UA increased the SOD level and reduced the levels of MDA and iron in the HG-induced DN cell model ($P < 0.001$). However, RO8191 treatment reduced the SOD level and promoted the levels of MDA and iron in the HG-induced DN cell model (all $P < 0.01$, Figure 8B–D). In addition, RO8191 further abolished the effect of UA on the levels of SOD, MDA, and iron (all $P < 0.01$, Figure 8B–D). Meanwhile, it was also discovered that 50 μM UA upregulated while RO8191 downregulated them GPX4 and

https://doi.org/10.2147/DDDT.S526554

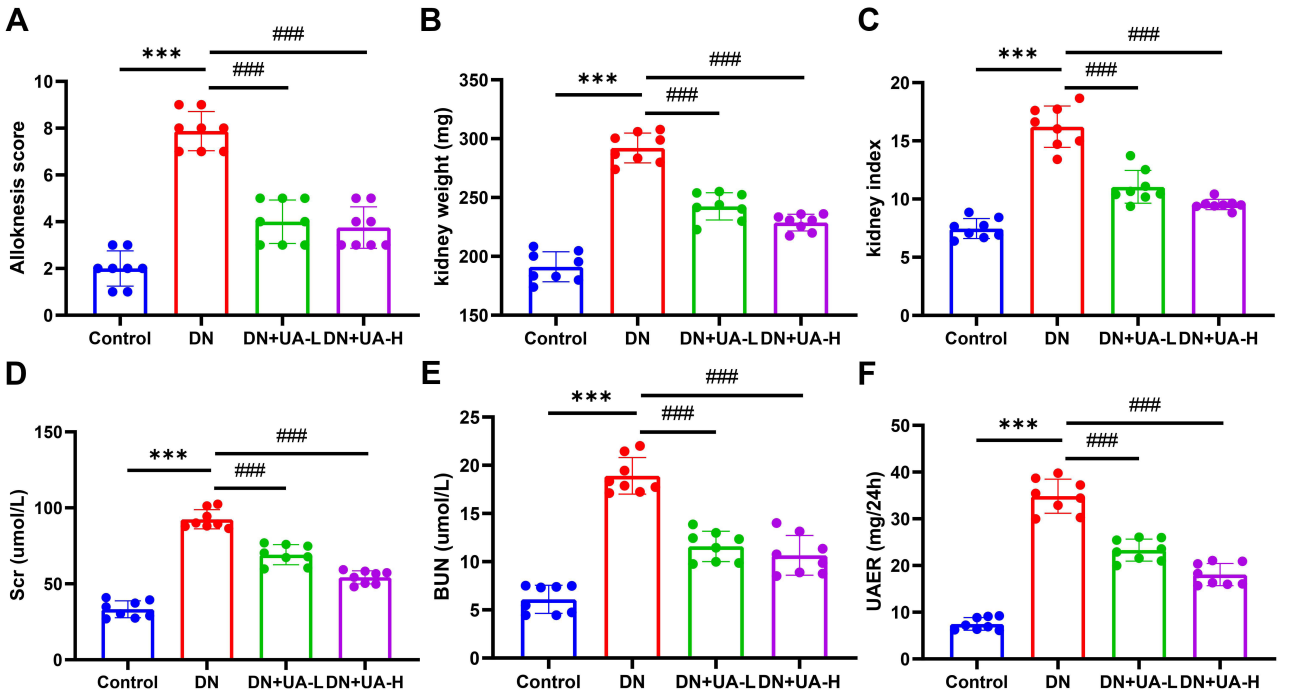

Figure 4 UA had an ameliorating role in the impaired renal function of DN mice. (**A**) The itch behaviors of all mice were documented using Alloknesis assessment. (**B**, **C**) The kidney weight (**B**) and kidney index (**C**) of all mice were documented. (**D**–**F**) The Scr (**D**), BUN (**E**), and UAER (**F**) of all mice were also determined using ELISA assay. Data are represented as mean ± SD (n=8). ***$P < 0.001$ vs Control; ###$P < 0.001$ vs DN.
Abbreviations: DN, diabetic nephropathy; UA, Ursolic acid; Scr, serum creatinine; BUN, blood urea nitrogen; UAER, urinary albumin excretion rate.

SLC7A11 in the HG-induced DN cell model (P < 0.001, Figure 8E). Furthermore, RO8191 offset the role of UA on GPX4 and SLC7A11 levels in the DN cell model (all P < 0.01, Figure 8E). These phenomena confirmed that the inhibitory role of UA in the ferroptosis of the DN cell model was realized by suppressing the JAK2/STAT3 pathway.

UA Inhibited the Ferroptosis of DN Mice by Inhibiting the JAK2/STAT3 Pathway

To further verify the above discovery in vivo, 2 mg/kg RO8191 and 100 mg/kg UA were applied to DN mice for 4 weeks, and the kidney tissues of mice were obtained for analysis. As shown in Figure 9A, the expression of p-JAK2 and p-STAT3 in kidney tissues was downregulated by UA and upregulated by RO8191 treatment, RO8191 further abolished the effect of UA on the levels of p-JAK2 and p-STAT3. Meanwhile, UA treatment increased SOD and reduced the levels of ROS, MDA, and iron in the kidney tissues of DN mice (P < 0.001, Figure 9B–E). RO8191 treatment decreased SOD while increasing the levels of ROS, MDA, and iron in kidney tissues of DN mice (all P < 0.01, Figure 9B–E). RO8191 treatment further abolished the role of UA in ROS, SOD, MDA, and iron (all P < 0.05, Figure 9B–E). Regarding the expression of genes related to ferroptosis, the results illustrated that the expression of GPX4 and SLC7A11 in the kidney tissues were upregulated by UA treatment and downregulated by RO8191 treatment (P < 0.001, Figure 9F). The role of UA in GPX4 and SLC7A11 expression was also offset by RO8191 treatment (all P < 0.01, Figure 9F). This evidence further proved that UA inhibits ferroptosis in DN mice by suppressing the JAK2/STAT3 pathway.

Discussion

As a serious complication of diabetes, DN affects one-third of diabetes patients and leads to a huge socioeconomic burden.[5] Kinds of therapeutic measures are selected to slow the progression of DN in clinical settings, but their efficacy is still insufficient and novel drugs need to be continuously developed. The effect of UA on ameliorating DN has been previously reported,[17] and the anti-hyperglycemic and renal function protective effect of UA on DN mice was also demonstrated in this study. This study also revealed that UA reduced ferroptosis and suppressed activation of the JAK2/STAT3 pathway in a DN mouse model and in cells. Moreover, the JAK2/STAT3 agonist abolished the role of UA in DN

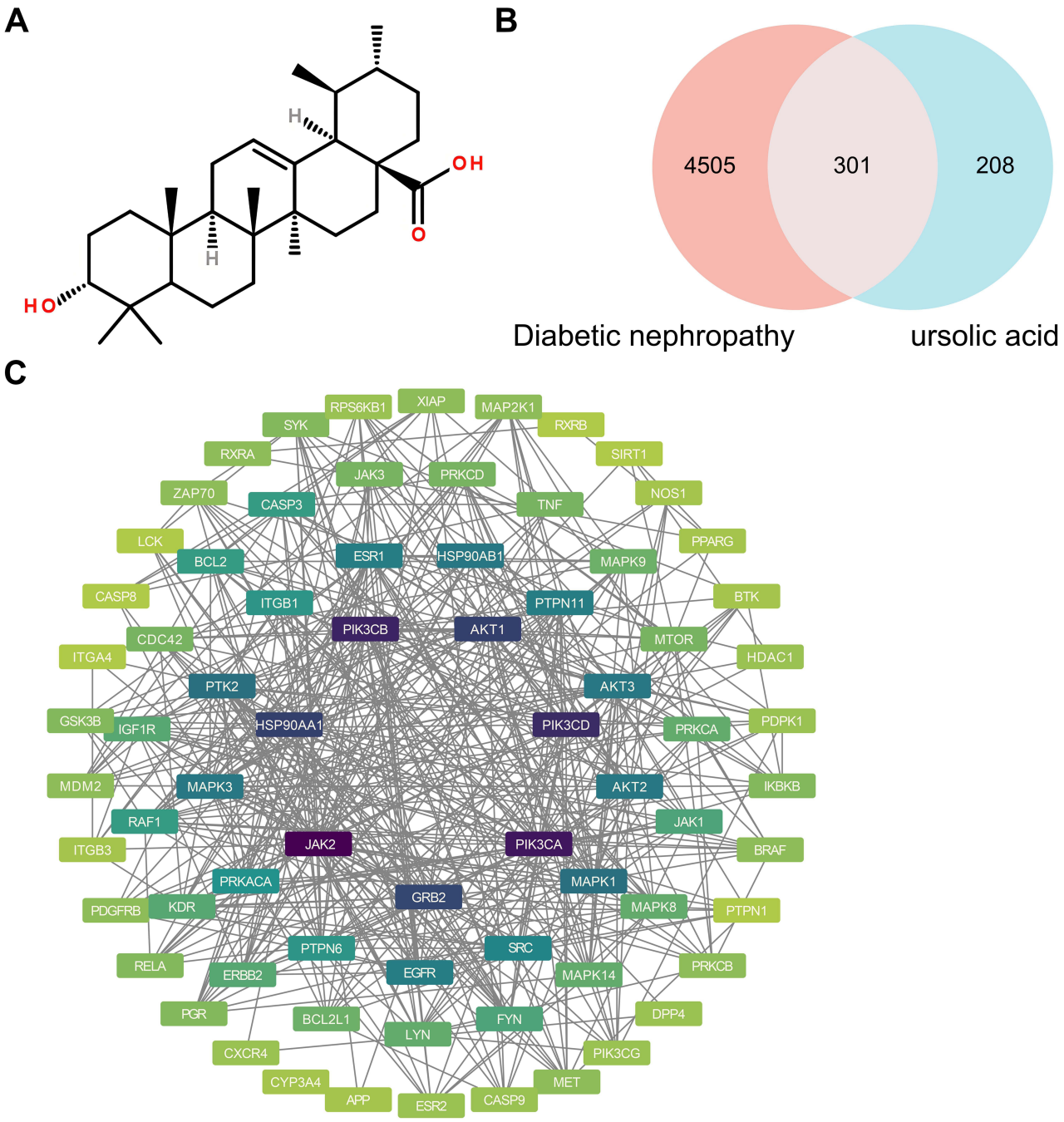

Figure 5 The potential targets of UA in treating DN. (**A**) UA molecular structure. (**B**) The potential targets of UA in treating DN were identified and exhibited with a Venn diagram by using the Venny 2.1 website. (**C**) The PPI network of the potential targets of UA in treating DN was constructed using the STRING platform and Cytoscape 3.9.1 software.

mice and cells. This study demonstrated that UA had a therapeutic effect on DN by suppressing JAK2/STAT3 pathway-mediated ferroptosis, providing a new theoretical basis for basic research and clinical treatment of DN.

As an active ingredient widely present in various plants, UA has been proven to have multiple pharmacological activities, including anti-tumor, anti-inflammatory, antioxidant, and antiviral.[41] The therapeutic benefits of UA in kidney disease have been previously proven; for example, UA ameliorates renal fibrosis in rats with chronic kidney disease,[42] and UA enhances NLRP3 degradation to improve lupus nephritis.[43] In addition, UA is reported to have a mitigating role in DN rats.[34] Similarly, our work also proved that UA had an anti-hyperglycemic and renal function protection effect on

https://doi.org/10.2147/DDDT.S526554

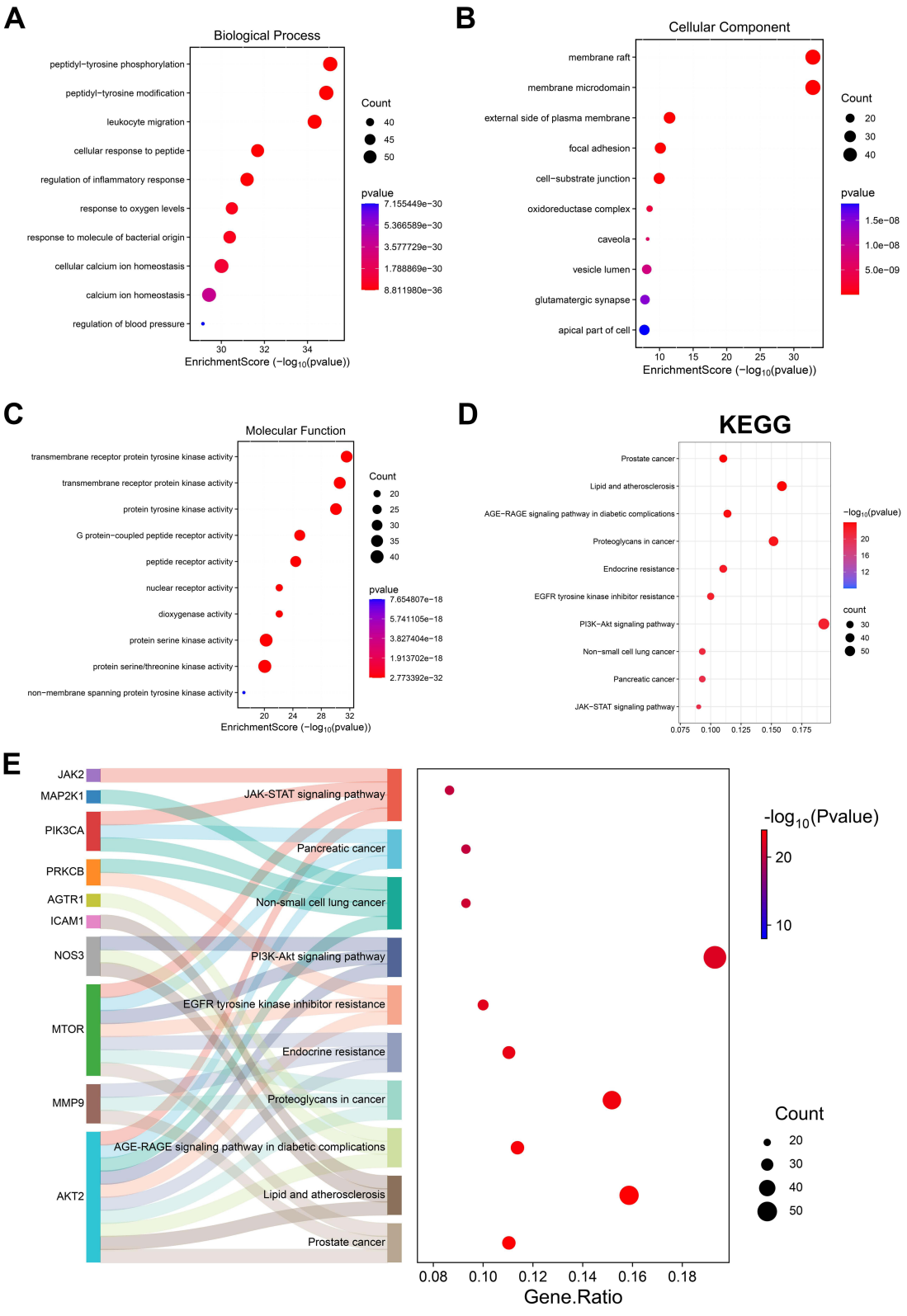

Figure 6 The role of UA in the treatment of DN might be realized through ferroptosis and the JAK/STAT signaling pathway. (**A**–**C**) With the help of the DAVID database and using R 4.2.0 software, GO function enrichment analysis was performed and the top 10 BP (**A**), the top 10 CC (**B**) and the top 10 MF (**C**) were depicted with bubble charts. (**D**) With the help of the DAVID database and using R 4.2.0 software, KEGG pathway enrichment analysis was performed, the top 10 pathways enriched in KEGG analysis were exhibited using bubble charts. (**E**) Detailed relationships between key genes and major pathways annotated by KEGG were shown by Sankey diagram.
Abbreviations: KEGG: Kyoto Encyclopedia of Genes and Genomes.

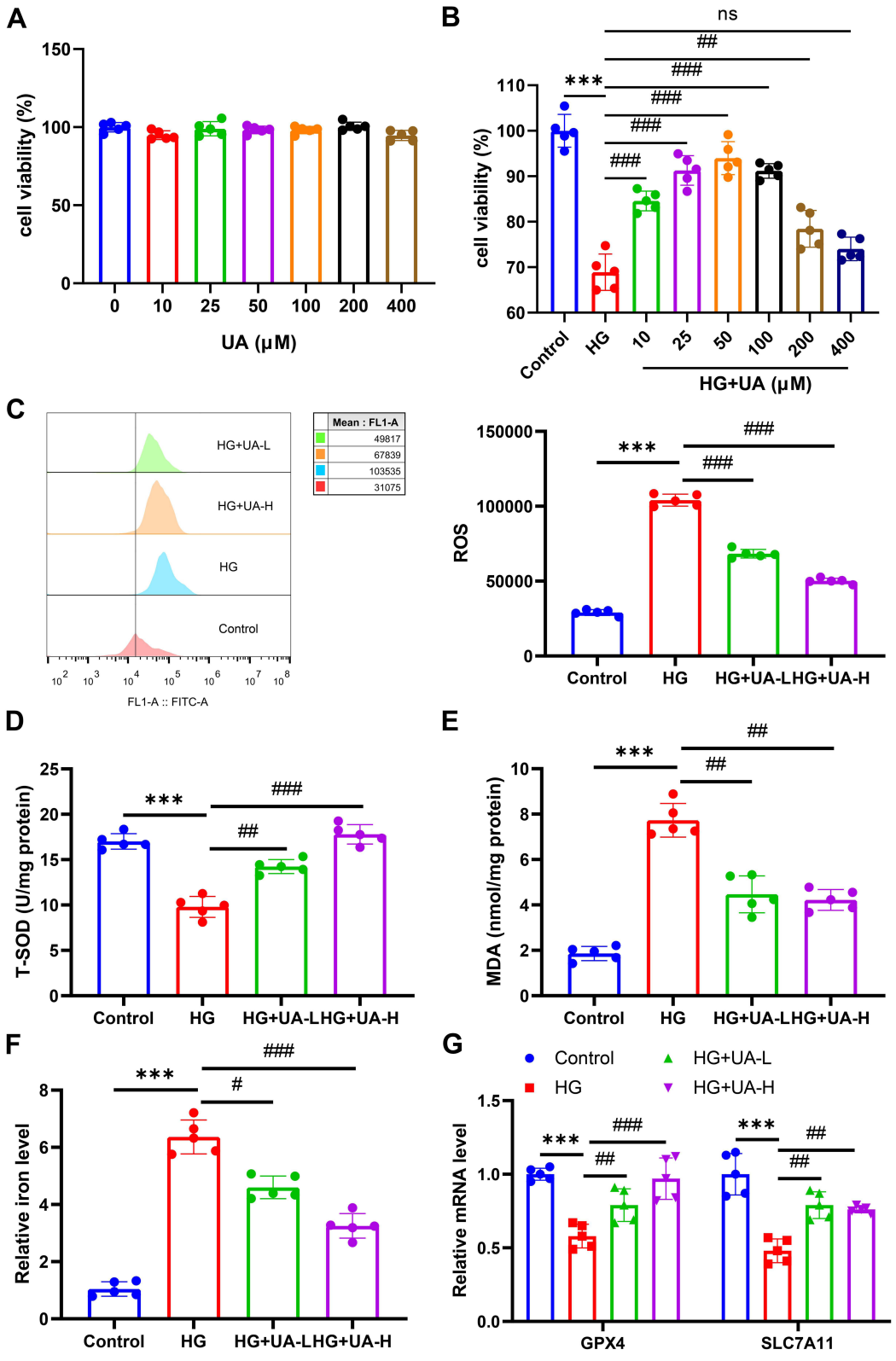

Figure 7 UA promoted the cell viability and inhibited the ferroptosis of DN cell model. (**A** and **B**) CCK-8 assay of UA on normal NRK-52E cells viability and HG-induced NRK-52E cells viability. (**C**) After being 30 mM HG induced for 48 h and 10 μM or 50 μM UA treated for 24 h, the ROS level in cells was determined using flow cytometry. (**D**–**F**) After being 30 mM HG induced for 48 h and 10 μM or 50 μM UA treated for 24 h, the levels of SOD (**D**), MDA (**E**), and iron (**F**) in cells were examined using ELISA assay. (**G**) After being 30 mM HG induced for 48 h and 10 μM or 50 μM UA treated for 24 h, the expressions of GPX4 and SLC7A11 in cells were quantified by qRT-PCR assay. Data are represented as mean ± SD (n=5). ns represents no significantly, ***$P < 0.001$ vs Control; $^{\#}P < 0.05$, $^{\#\#}P < 0.01$, $^{\#\#\#}P < 0.001$ vs HG.

Abbreviations: UA, Ursolic acid; HG, high glucose; ROS, reactive oxygen species; SOD, superoxide dismutase; MDA, malondialdehyde; GPX4, Glutathione peroxidase 4; SLC7A11, solute carrier family 7 member 11.

https://doi.org/10.2147/DDDT.S526554

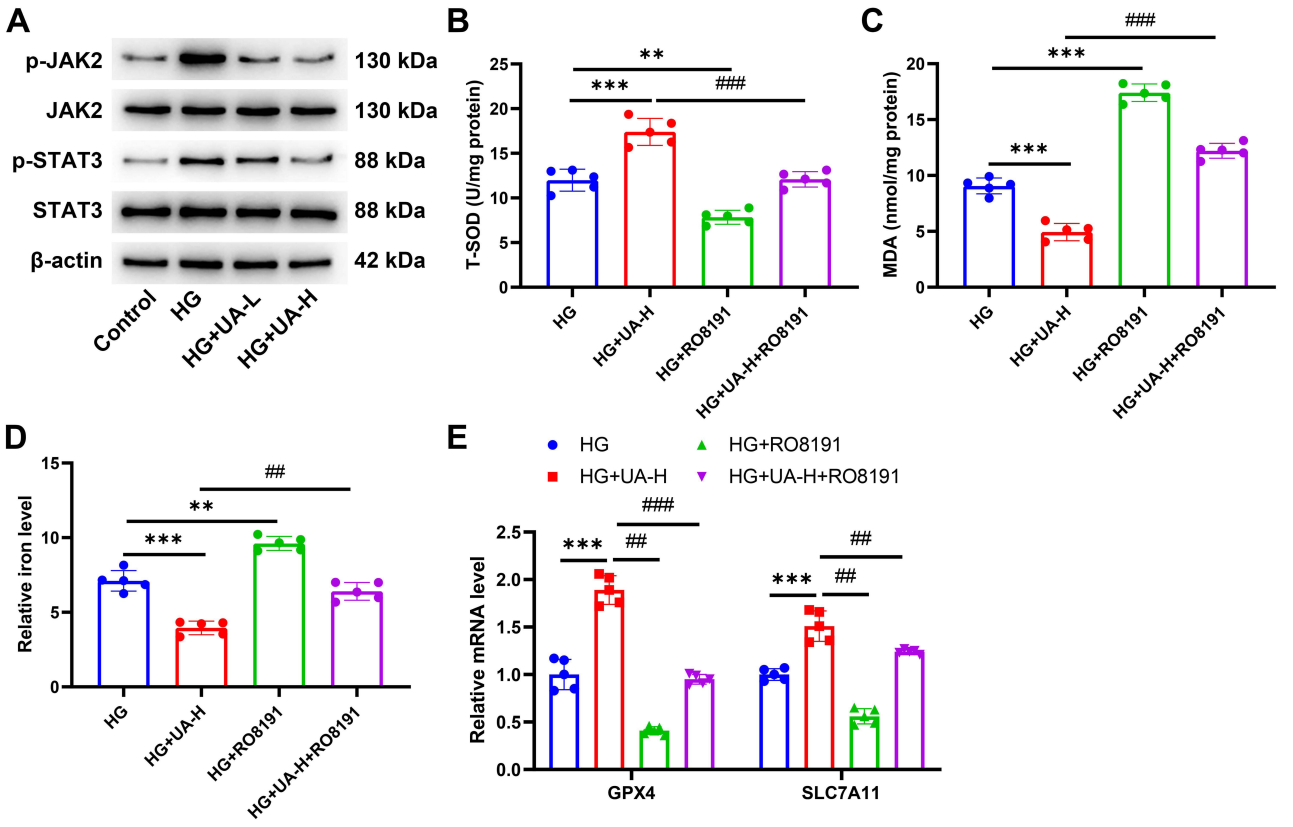

Figure 8 UA inhibited the ferroptosis of DN cell model by inhibiting the JAK2/STAT3 pathway. (**A**) After being 30 mM HG induced for 48 h and 10 μM or 50 μM UA treated for 24 h, the transduction of the JAK2/STAT3 pathway in NRK-52E cells was determined by Western blot. (**B**–**E**) Being further treated with 50 μM UA and 2 μM RO8191 for 24 h after 30 mM HG induced for 48 h, the levels of SOD, MDA, and iron in cells were examined using ELISA assay (**B**–**D**), and the gene levels of GPX4 and SLC7A11 in cells were quantified by qRT-PCR assay (**E**). Data are represented as mean ± SD (n=5). $^{**}P < 0.01$, $^{***}P < 0.001$ vs HG; $^{\#\#}P < 0.01$, $^{\#\#\#}P < 0.001$ vs HG+UA-H.
Abbreviations: UA, Ursolic acid; HG, high glucose; SOD, superoxide dismutase; MDA, malondialdehyde; GPX4, Glutathione peroxidase 4; SLC7A11, solute carrier family 7 member 11.

DN mice. UA alleviates DN by suppressing oxidative stress.[17] Oxidative stress is the process of excessive ROS accumulation resulting from the imbalance between antioxidants (such as SOD) and oxidants (such as MDA), which further contributes to oxidative damage.[1] In our study, UA was found to increase SOD and decrease ROS and MDA in DN cell models and mice, further proving the antioxidant role in DN, while the deep regulatory mechanism requires further exploration.

The abnormal accumulation of ROS and the bring-out of oxidative stress participate in the ferroptosis process, which is an iron-dependent form of cell death caused by intracellular iron deposition, resulting in the accumulation of harmful lipid peroxides.[44] Numbers research suggested that ferroptosis is closely associated with the complications of diabetes. In type 2 diabetes, ferroptosis not only destroys the secretion of insulin and induces ROS production, but also gives rise to the complications of diabetes including diabetic cardiomyopathy,[45] diabetic retinopathy,[46] diabetic wound healing disorders,[47] as well as DN.[48] GPX4 and SLC7A11, the members of the solute carrier family and markers of ferroptosis, regulate the entry and exit of cystine and glutamate intracellular, and the reduction of GPX4 and SLC7A11, leading to the damage of cell antioxidant ability and final causing the aggravating of DN.[49] In this study, the iron level was increased and the levels of GPX4 and SLC7A11 decreased in DN mice and cells, indicating that ferroptosis is enhanced in DN mice and cells. The treatment for ferroptosis have a positive effect on DN treatment by preventing inflammation and fibrosis caused by specific cell death patterns.[50] Recent research has begun to establish a connection between natural products and ferroptosis in DN.[51] For instance, Ginkgolide B from Ginkgo biloba improves the DN by inhibiting oxidative stress and ferroptosis.[52] Glabridin, a bioactive component of licorice, ameliorates diabetic nephropathy by regulating ferroptosis and the VEGF/Akt/ERK pathways.[24] The inhibiting role of UA in ferroptosis is discovered in

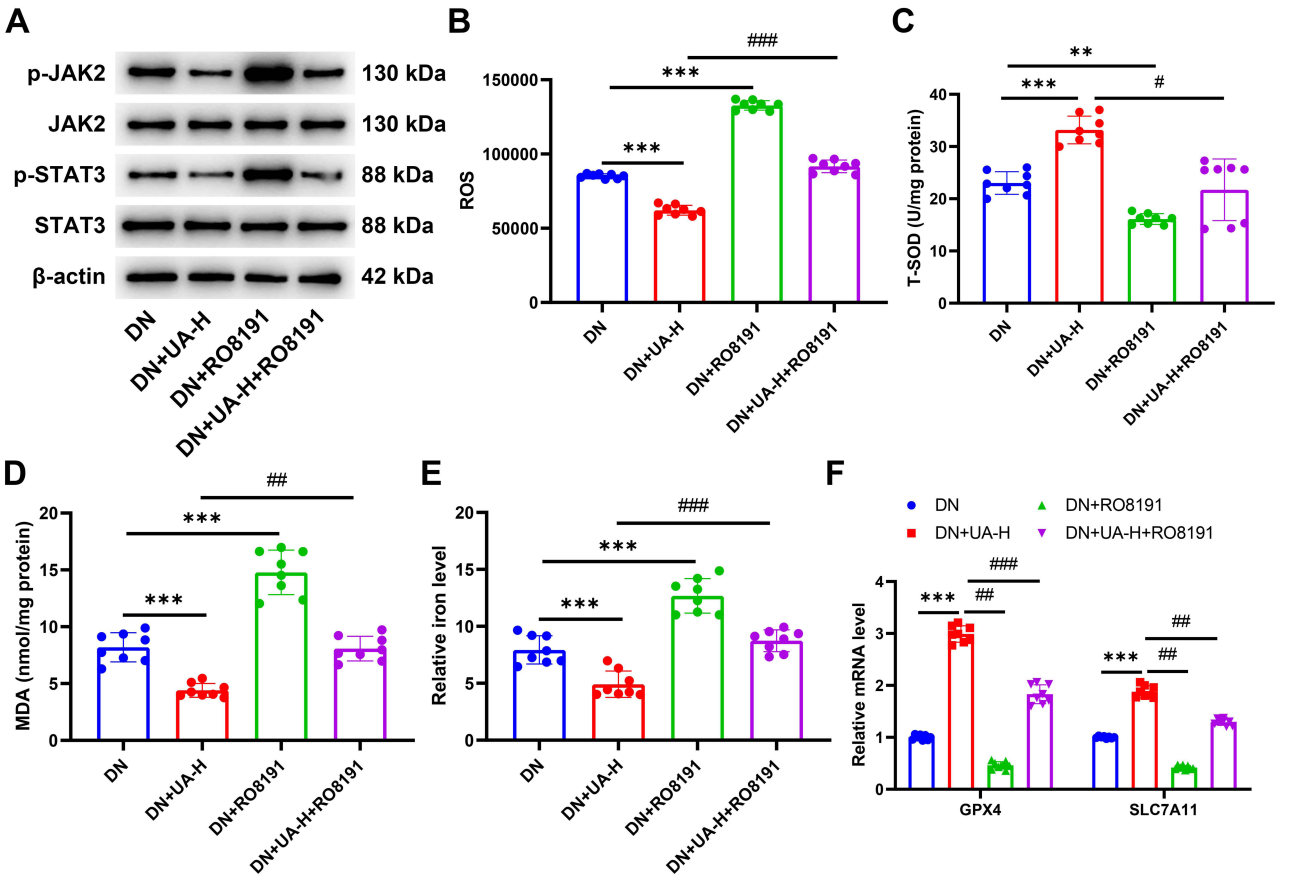

Figure 9 UA inhibited the ferroptosis of DN mice by inhibiting the JAK2/STAT3 pathway. (**A**) After the DN mice were treated with 2 mg/kg RO8191 and 100 mg/kg UA for 4 weeks, the transduction of JAK2/STAT3 pathway in mouse kidney tissues was detected by Western blot. (**B**–**E**) The levels of ROS (**B**), SOD (**C**), MDA (**D**), and iron (**E**) in mouse kidney tissues were determined using ELISA assays. (**F**) The expressions of ferroptosis-related genes were quantified using qRT-PCR assay. Data are represented as mean ± SD (n=8). $^{**}P < 0.01$, $^{***}P < 0.001$ vs DN; $^{\#}P < 0.05$, $^{\#\#}P < 0.01$, $^{\#\#\#}P < 0.001$ vs DN+UA-H.

Abbreviations: DN, diabetic nephropathy; UA, Ursolic acid; ROS, reactive oxygen species; SOD, superoxide dismutase; MDA, malondialdehyde; GPX4, Glutathione peroxidase 4; SLC7A11, solute carrier family 7 member 11.

alcoholic liver injury.[53] Hyaluronic acid-coated UA nanoparticles was found to inhibit ferroptosis level of temporal lobe cortex in mice.[54] UA upregulated the expression of GPX4 and SLC7A11 in the liver and exerted hepatoprotective effects by inhibiting alcohol-induced ferroptosis.[53] However, the detailed mechanism by which it inhibits ferroptosis, especially in DN, is largely elusive. In the current study, through network pharmacology, ferroptosis was found to be enriched by UA targets in DN. For the first time, it was discovered that UA downregulated iron levels and upregulated GPX4 and SLC7A11 expression in a DN mouse model and cell lines, demonstrating that UA reduced ferroptosis.

In addition to ferroptosis, we also locked JAK2/STAT3 signaling, which was enriched by the targets of UA in DN, with the aid of network pharmacology in the current study. JAK2/STAT3 signaling, as a central communication node in cells, exerts a crucial effect on a wide range of pathophysiological activities, such as cell differentiation, cell proliferation, immune response, and so on.[55] In recent years, the first time that UA promoted the transcription of JAK2 and STAT3 are upregulated by the DN model, and inhibiting the JAK2/STAT3 pathway in DN.[56,57] Similarly, we demonstrated for the first time that UA promoted the transcription of GPX4 and SLC7A11 by inhibiting the JAK2/STAT3 pathway in DN. Recent studies suggest that JAK/STAT signaling influences ferroptosis by modulating cellular antioxidant defenses, such as the regulation of GPX4, which can suppress lipid peroxidation and protect against ferroptotic cell death.[58] Some researchers also found that IFN-γ activated the JAK1-2/STAT1 signaling cascade, which downregulated the expression of System Xc−components SLC7A11 and SLC3A2.[59] In the field of TCM research, Erianin has been proven to inhibit the expression of SLC7A11 and GPX4 by activating the JAK2/STAT3 signaling pathway.[60] Thus, we hypothesized if the role of UA in improving DN was realized by JAK2/STAT3 signaling-mediated ferroptosis.

https://doi.org/10.2147/DDDT.S526554

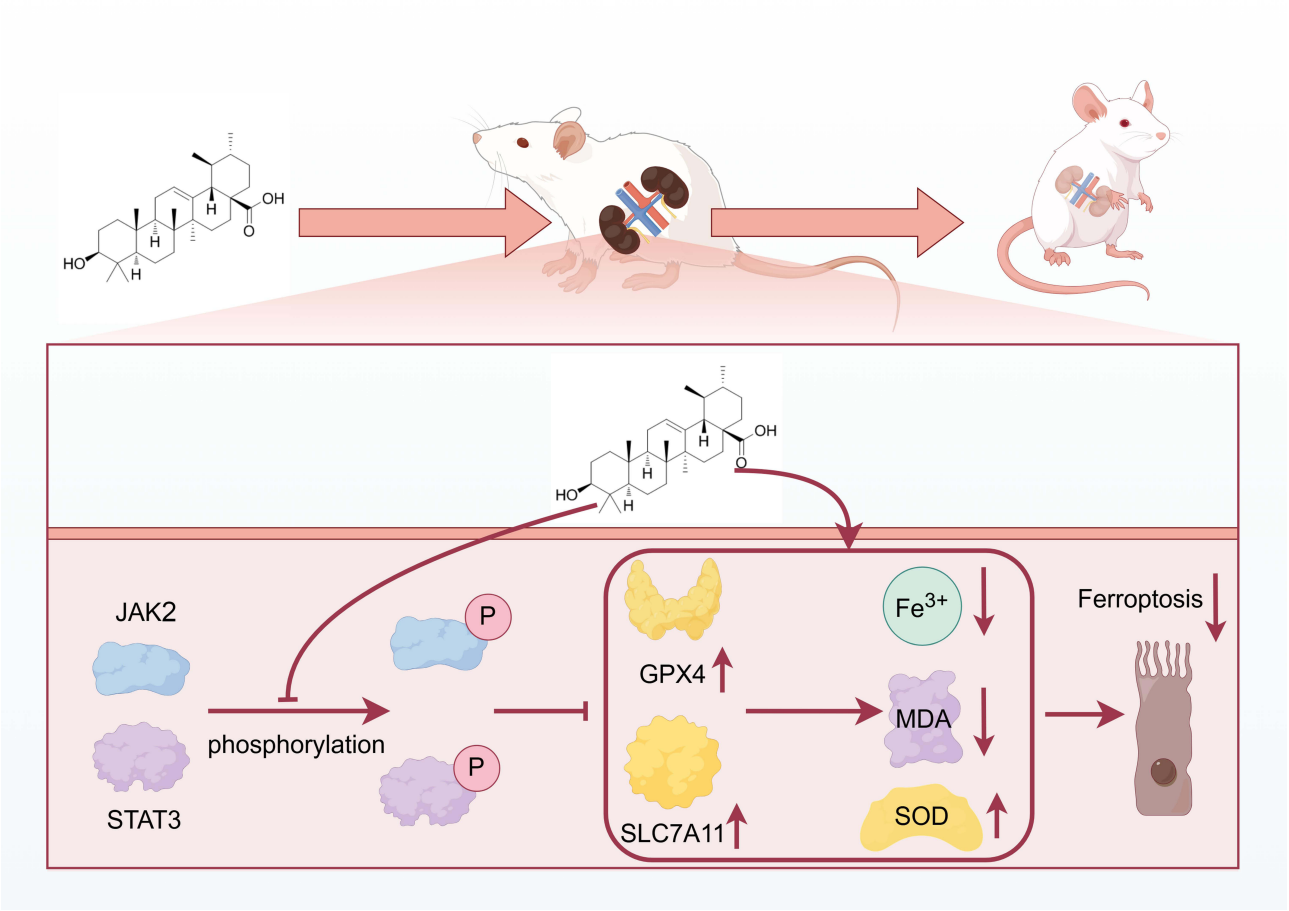

Figure 10 Schematic model of ursolic acid plays an amelioratory role in diabetic nephropathy by suppressing the JAK2/STAT3 pathway-mediated ferroptosis.
Abbreviations: JAK, Janus Kinase; STAT, signal transducer and activator of transcription; SOD, superoxide dismutase; MDA, malondialdehyde; GPX4, Glutathione peroxidase 4; SLC7A11, solute carrier family 7 member 11; P, Phosphorylation; ↑, up-regulated; ↓, up-regulated.

Subsequently, the JAK2 agonist RO8191 was used in this study, and we found that RO8191 offset the function of UA in inhibiting oxidative stress and ferroptosis. Previous reports and our results suggest that UA ameliorates DN at least in part by inhibiting JAK2/STAT3-driven ferroptosis.

Nevertheless, this study has some limitations. First, direct targets of UA in DN have not been verified and the interactions with other pathways (for instance NRF2) have not been explored, and the validation of targets should be included in the proposed directions for future research. Second, this study only demonstrated the role of the JAK2/STAT3 signaling pathway in the improvement of DN. Additional pathways and targets need to be verified in future studies. Third, the relatively small sample size and shorter drug treatment time may reduce the power to detect subtle effects in the present study.

Further in-depth investigation is warranted. First, the conclusions obtained in this study should be verified using various animal models of DN. Prolonged treatment time of UA and increased dose to evaluate the safety, efficacy, and optimal dosing regimens more accurately. For preclinical research, organoids and humanized mouse models that closely mimic human DN conditions should be used to better understand UA's therapeutic mechanisms of UA. Finally, studies on the safety, efficacy, and pharmacokinetics of UA should be conducted in clinical trials. These in-depth explorations are conducive to clarifying the molecular mechanism of UA in DN treatment.

Conclusion

In conclusion, this study revealed that UA may be a natural candidate for JAK/STAT3-targeted therapy. UA had the effect on suppressed hyperglycemia, protected renal function, reduced ferroptosis, and inactivated the JAK2/STAT3 pathway in a DN model. In addition, activation of the JAK2-STAT3 pathway offsets the role of UA in DN (Figure 10).

However, further validation of the long-term efficacy and safety of UA in chronic DN models is required. Our research provides a new perspective on the application of UA and demonstrates considerable potential for clinical translation in the management of patients with UA. Further clinical research is helpful for clarifying the best treatment approach for UA in DN and provides an important reference for clinical transformation.

Data Sharing Statement

All the results are presented in the article. Further inquiries can be directed to the corresponding authors.

Supplementary Materials

The original contributions presented in the study are included in the article/supplementary material, and further inquiries can be directed to the corresponding author.

Ethical Approval

All the animal procedures in this study were performed in accordance with the Guidelines for Care and Use of Laboratory Animals of the National Institutes of Health. Approval for all animal experiments was obtained from the Ethics Committee of Jiaxing Traditional Chinese Medicine Hospital (Approval number: JUMC2025-029).

Funding

This study was supported by the The university-level scientific research project of Zhejiang University of Traditional Chinese Medicine and the specialized scientific research project of the affiliated hospital (2024FSYYZQ18).

Disclosure

The authors report no conflicts of interest in this work.

References

1. Ataei M, Gumpricht E, Kesharwani P, Jamialahmadi T, Sahebkar A. Recent advances in curcumin-based nanoformulations in diabetes. *J Drug Target*. 2023;31(7):671–684. doi:10.1080/1061186x.2023.2229961
2. Li Y, Su X, Ye Q, et al. The predictive value of diabetic retinopathy on subsequent diabetic nephropathy in patients with type 2 diabetes: a systematic review and meta-analysis of prospective studies. *Ren Fail*. 2021;43(1):231–240. doi:10.1080/0886022x.2020.1866010
3. Ji JL, Shi HM, Li ZL, et al. Satellite cell-derived exosome-mediated delivery of microRNA-23a/27a/26a cluster ameliorates the renal tubulointerstitial fibrosis in mouse diabetic nephropathy. *Acta pharmacologica Sinica*. 2023;44(12):2455–2468. doi:10.1038/s41401-023-01140-4
4. Wang B, Xiong Y, Deng X, et al. The role of intercellular communication in diabetic nephropathy. *Front Immunol*. 2024;15:1423784. doi:10.3389/fimmu.2024.1423784
5. Cheng G, Liu Y, Guo R, Wang H, Zhang W, Wang Y. Molecular mechanisms of gut microbiota in diabetic nephropathy. *Diabetes Res Clin Pract*. 2024;213:111726. doi:10.1016/j.diabres.2024.111726
6. Peng Z, Liang Y, Liu X, Shao J, Hu N, Zhang X. New insights into the mechanisms of diabetic kidney disease: role of circadian rhythm and Bmal1. *Biomed Pharmacother*. 2023;166:115422. doi:10.1016/j.biopha.2023.115422
7. Zhou D, Zhou T, Tang S, et al. Network pharmacology combined with Mendelian randomization analysis to identify the key targets of renin-angiotensin-aldosterone system inhibitors in the treatment of diabetic nephropathy. *Front Endocrinol*. 2024;15:1354950. doi:10.3389/fendo.2024.1354950
8. Dong W, Zhang H, Zhao C, Luo Y, Chen Y. Silencing of miR-150-5p ameliorates diabetic nephropathy by targeting SIRT1/p53/AMPK pathway. *Front Physiol*. 2021;12:624989. doi:10.3389/fphys.2021.624989
9. Liu XJ, Hu XK, Yang H, et al. A review of traditional Chinese medicine on treatment of diabetic nephropathy and the involved mechanisms. *Am J Chin Med*. 2022;50(7):1739–1779. doi:10.1142/s0192415x22500744
10. Qiu L, Wang Y, Wang Y, et al. Ursolic acid ameliorated neuronal damage by restoring microglia-activated MMP/TIMP imbalance in vitro. *Drug Des Devel Ther*. 2023;17:2481–2493. doi:10.2147/dddt.S411408
11. Shi Y, Liu J, Hou M, et al. Ursolic acid improves necroptosis via STAT3 signaling in intestinal ischemia/reperfusion injury. *Int Immunopharmacol*. 2024;138:112463. doi:10.1016/j.intimp.2024.112463
12. Wan Y, Zhang W, Huang C, et al. Ursolic acid alleviates Kupffer cells pyroptosis in liver fibrosis by the NOX2/NLRP3 inflammasome signaling pathway. *Int Immunopharmacol*. 2022;113(Pt A):109321. doi:10.1016/j.intimp.2022.109321
13. Dai Y, Sun L, Tan Y, et al. Recent progress in the development of ursolic acid derivatives as anti-diabetes and anti-cardiovascular agents. *Chem Biol Drug Des*. 2023;102(6):1643–1657. doi:10.1111/cbdd.14347
14. Khwaza V, Oyedeji OO, Aderibigbe BA. Ursolic acid-based derivatives as potential anti-cancer agents: an update. *Int J Mol Sci*. 2020;21(16):5920. doi:10.3390/ijms21165920
15. Zou J, Lin J, Li C, et al. Ursolic acid in cancer treatment and metastatic chemoprevention: from synthesized derivatives to nanoformulations in preclinical studies. *Curr Cancer Drug Tar*. 2019;19(4):245–256. doi:10.2174/1568009618666181016145940

16. Wu X, Li H, Wan Z, et al. The combination of ursolic acid and empagliflozin relieves diabetic nephropathy by reducing inflammation, oxidative stress and renal fibrosis. *Biomed Pharmacother*. 2021;144:112267. doi:10.1016/j.biopha.2021.112267
17. Xu HL, Wang XT, Cheng Y, et al. Ursolic acid improves diabetic nephropathy via suppression of oxidative stress and inflammation in streptozotocin-induced rats. *Biomed Pharmacother*. 2018;105:915–921. doi:10.1016/j.biopha.2018.06.055
18. Liu Y, Zheng JY, Wei ZT, et al. Therapeutic effect and mechanism of combination therapy with ursolic acid and insulin on diabetic nephropathy in a type I diabetic rat model. *Front Pharmacol*. 2022;13:969207. doi:10.3389/fphar.2022.969207
19. Li L, Dai Y, Ke D, et al. Ferroptosis: new insight into the mechanisms of diabetic nephropathy and retinopathy. *Front Endocrinol*. 2023;14:1215292. doi:10.3389/fendo.2023.1215292
20. Li Y, Sun M, Cao F, et al. The ferroptosis inhibitor liproxstatin-1 ameliorates lps-induced cognitive impairment in mice. *Nutrients*. 2022;14(21). doi:10.3390/nu14214599
21. Wu Q, Huang F. Targeting ferroptosis as a prospective therapeutic approach for diabetic nephropathy. *Ann Med*. 2024;56(1):2346543. doi:10.1080/07853890.2024.2346543
22. Park JE, Lee H, Kim SY, Lim Y. Lespedeza bicolor extract ameliorated renal inflammation by regulation of NLRP3 inflammasome-associated hyperinflammation in type 2 diabetic mice. *Antioxidants*. 2020;9(2):148. doi:10.3390/antiox9020148
23. Wei M, Liu X, Tan Z, Tian X, Li M, Wei J. Ferroptosis: a new strategy for Chinese herbal medicine treatment of diabetic nephropathy. *Front Endocrinol*. 2023;14:1188003. doi:10.3389/fendo.2023.1188003
24. Tan H, Chen J, Li Y, et al. Glabridin, a bioactive component of licorice, ameliorates diabetic nephropathy by regulating ferroptosis and the VEGF/Akt/ERK pathways. *Mol Med*. 2022;28(1):58. doi:10.1186/s10020-022-00481-w
25. Zhang S, Zhang S, Wang H, Chen Y. Vitexin ameliorated diabetic nephropathy via suppressing GPX4-mediated ferroptosis. *Eur J Pharmacol*. 2023;951:175787. doi:10.1016/j.ejphar.2023.175787
26. Liu Q, Liang X, Liang M, Qin R, Qin F, Wang X. Ellagic acid ameliorates renal ischemic-reperfusion injury through NOX4/JAK/STAT signaling pathway. *Inflammation*. 2020;43(1):298–309. doi:10.1007/s10753-019-01120-z
27. Yu C, Zhang J, Pei J, et al. IL-13 alleviates acute kidney injury and promotes regeneration via activating the JAK-STAT signaling pathway in a rat kidney transplantation model. *Life Sci*. 2024;341:122476. doi:10.1016/j.lfs.2024.122476
28. Li X, Wang Z, Zhang S, Yao Q, Chen W, Liu F. Ruxolitinib induces apoptosis of human colorectal cancer cells by downregulating the JAK1/2-STAT1-Mcl-1 axis. *Oncology Letters*. 2021;21(5):352. doi:10.3892/ol.2021.12613
29. Zhang Z, Deng S, Shi Q. Isoliquiritigenin attenuates high glucose-induced proliferation, inflammation, and extracellular matrix deposition in glomerular mesangial cells by suppressing JAK2/STAT3 pathway. *Naunyn-Sch Arch Pharmacol*. 2024;397(1):123–131. doi:10.1007/s00210-023-02598-z
30. Wen W, Sun J, Ma Y, et al. Renal protective effect of boeravinone b against diabetic nephropathy rats via inhibition of the inflammatory and JAK2/STAT3 signalling pathway. *Cell Journal*. 2024;26(6):351–360. doi:10.22074/cellj.2024.2017978.1468
31. Zhang Z, He Y, Liu H, et al. NLRP3 regulates ferroptosis via the JAK2/STAT3 pathway in asthma inflammation: insights from in vivo and in vitro studies. *Int Immunopharmacol*. 2024;143(Pt 2):113416. doi:10.1016/j.intimp.2024.113416
32. Kim K, Shin EA, Jung JH, et al. Ursolic acid induces apoptosis in colorectal cancer cells partially via upregulation of MicroRNA-4500 and Inhibition of JAK2/STAT3 phosphorylation. *Int J Mol Sci*. 2018;20(1):114. doi:10.3390/ijms20010114
33. Li Y, Hou JG, Liu Z, et al. Alleviative effects of 20(R)-Rg3 on HFD/STZ-induced diabetic nephropathy via MAPK/NF-κB signaling pathways in C57BL/6 mice. *J Ethnopharmacol*. 2021;267:113500. doi:10.1016/j.jep.2020.113500
34. Li J, Li N, Yan S, et al. Ursolic acid alleviates inflammation and against diabetes-induced nephropathy through TLR4-mediated inflammatory pathway. *Mol Med Rep*. 2018;18(5):4675–4681. doi:10.3892/mmr.2018.9429
35. Zheng Y, Zhao L, Xiong Z, et al. Ursolic acid targets secreted phosphoprotein 1 to regulate Th17 cells against metabolic dysfunction-associated steatotic liver disease. *Clin Mol Hepatol*. 2024;30(3):449–467. doi:10.3350/cmh.2024.0047
36. Tian C, Li J, Bao Y, et al. Ursolic acid ameliorates obesity of mice fed with high-fat diet via alteration of gut microbiota and amino acid metabolism. *Front Microbiol*. 2023;14:1183598. doi:10.3389/fmicb.2023.1183598
37. Xu Y, Tan X, Yang Q, Fang Z, Chen W. Akkermansia muciniphila outer membrane protein regulates recruitment of CD8(+) T cells in lung adenocarcinoma and through JAK-STAT signalling pathway. *Microb Biotechnol*. 2024;17(7):e14522. doi:10.1111/1751-7915.14522
38. Cheng RX, Feng Y, Liu D, et al. The role of Na(v)1.7 and methylglyoxal-mediated activation of TRPA1 in itch and hypoalgesia in a murine model of type 1 diabetes. *Theranostics*. 2019;9(15):4287–4307. doi:10.7150/thno.36077
39. Sherkhane B, Yerra VG, Sharma A, et al. Nephroprotective potential of syringic acid in experimental diabetic nephropathy: focus on oxidative stress and autophagy. *Indian J Pharmacol*. 2023;55(1):34–42. doi:10.4103/ijp.ijp_671_22
40. Gilyazova I, Ivanova E, Sinelnikov M, et al. The potential of miR-153 as aggressive prostate cancer biomarker. *Noncoding RNA Res*. 2023;8(1):53–59. doi:10.1016/j.ncrna.2022.10.002
41. Al-Kuraishy HM, Al-Gareeb AI, Negm WA, Alexiou A, Batiha GE. Ursolic acid and SARS-CoV-2 infection: a new horizon and perspective. *Inflammopharmacology*. 2022;30(5):1493–1501. doi:10.1007/s10787-022-01038-3
42. Thakur R, Sharma A, Lingaraju MC, et al. Ameliorative effect of ursolic acid on renal fibrosis in adenine-induced chronic kidney disease in rats. *Biomed Pharmacother*. 2018;101:972–980. doi:10.1016/j.biopha.2018.02.143
43. Chen L, Li F, Ni JH, et al. Ursolic acid alleviates lupus nephritis by suppressing SUMO1-mediated stabilization of NLRP3. *Phytomedicine*. 2024;130:155556. doi:10.1016/j.phymed.2024.155556
44. Li J, Li L, Zhang Z, et al. Ferroptosis: an important player in the inflammatory response in diabetic nephropathy. *Front Immunol*. 2023;14:1294317. doi:10.3389/fimmu.2023.1294317
45. Wang X, Chen X, Zhou W, et al. Ferroptosis is essential for diabetic cardiomyopathy and is prevented by sulforaphane via AMPK/NRF2 pathways. *Acta Pharm Sin B*. 2022;12(2):708–722. doi:10.1016/j.apsb.2021.10.005
46. Luo L, Cai Y, Jiang Y, et al. Pipecolic acid mitigates ferroptosis in diabetic retinopathy by regulating GPX4-YAP signaling. *Biomed Pharmacother*. 2023;169:115895. doi:10.1016/j.biopha.2023.115895
47. Wei X, Liu M, Zheng Z, et al. Defective NCOA4-dependent ferroptosis in senescent fibroblasts retards diabetic wound healing. *Cell Death Discov*. 2023;9(1):138. doi:10.1038/s41420-023-01437-7
48. Li S, Zheng L, Zhang J, Liu X, Wu Z. Inhibition of ferroptosis by up-regulating Nrf2 delayed the progression of diabetic nephropathy. *Free Radic Biol Med*. 2021;162:435–449. doi:10.1016/j.freeradbiomed.2020.10.323

49. Zhang X, Li X. Abnormal iron and lipid metabolism mediated ferroptosis in kidney diseases and its therapeutic potential. *Metabolites*. 2022;12(1). doi:10.3390/metabo12010058
50. Wang Y, Bi R, Quan F, et al. Ferroptosis involves in renal tubular cell death in diabetic nephropathy. *Eur J Pharmacol*.. 2020;888:173574. doi:10.1016/j.ejphar.2020.173574
51. Zheng K, Dong Y, Yang R, Liang Y, Wu H, He Z. Regulation of ferroptosis by bioactive phytochemicals: implications for medical nutritional therapy. *Pharmacol Res*. 2021;168:105580. doi:10.1016/j.phrs.2021.105580
52. Chen J, Ou Z, Gao T, et al. Ginkgolide B alleviates oxidative stress and ferroptosis by inhibiting GPX4 ubiquitination to improve diabetic nephropathy. *Biomed Pharmacother*. 2022;156:113953. doi:10.1016/j.biopha.2022.113953
53. Zhou L, Xiao M, Li Y, Chitrakar B, Sheng Q, Zhao W. Ursolic acid ameliorates alcoholic liver injury through attenuating oxidative stress-mediated ferroptosis and modulating gut microbiota. *J Agricult Food Chem*. 2024;72(38):21181–21192. doi:10.1021/acs.jafc.4c04762
54. Li Y, Zhu X, Xiong W, et al. Brain-targeted ursolic acid nanoparticles for anti-ferroptosis therapy in subarachnoid hemorrhage. *J Nanobiotechnol*. 2024;22(1):641. doi:10.1186/s12951-024-02866-x
55. Zhang JQ, Li R, Dong XY, et al. Design, synthesis and structure-activity relationship studies of meridianin derivatives as novel JAK/STAT3 signaling inhibitors. *Int J Mol Sci*. 2022;23(4). doi:10.3390/ijms23042199
56. Gao C, Fei X, Wang M, Chen Q, Zhao N. Cardamomin protects from diabetes-induced kidney damage through modulating PI3K/AKT and JAK/STAT signaling pathways in rats. *Int Immunopharmacol*. 2022;107:108610. doi:10.1016/j.intimp.2022.108610
57. Ren Y, Yu M, Zheng D, He W, Jin J. Lysozyme promotes renal fibrosis through the JAK/STAT3 signal pathway in diabetic nephropathy. *Arch Med Sci*. 2024;20(1):233–247. doi:10.5114/aoms/170160
58. Wu D, Wang Z, Zhang Y, et al. IL15RA-STAT3-GPX4/ACSL3 signaling leads to ferroptosis resistance in pancreatic cancer. *Acta biochimica et biophysica Sinica*. 2024;57(3):389–402. doi:10.3724/abbs.2024153
59. Cao T, Zhou J, Liu Q, et al. Interferon-γ induces salivary gland epithelial cell ferroptosis in Sjogren's syndrome via JAK/STAT1-mediated inhibition of system Xc(). *Free Radical Biol Med*. 2023;205:116–128. doi:10.1016/j.freeradbiomed.2023.05.027
60. Chen L, Sun R, Fang K. Erianin inhibits tumor growth by promoting ferroptosis and inhibiting invasion in hepatocellular carcinoma through the JAK2/STAT3/SLC7A11 pathway. *Pathol Int*. 2024;74(3):119–128. doi:10.1111/pin.13403